Quantum metrology with a transmon qutrit

A. R. Shlyakhov,[1] V. V. Zemlyanov,[1] M. V. Suslov,[1] A. V. Lebedev,[1,2,*] G. S. Paraoanu,[3] G. B. Lesovik,[1] and G. Blatter[2]

[1]*Moscow Institute of Physics and Technology, Institutskii per. 9, Dolgoprudny, 141700 Moscow District, Russia*

[2]*Theoretische Physik, Wolfgang-Pauli-Strasse 27, ETH Zurich, CH-8093 Zürich, Switzerland*

[3]*Low Temperature Laboratory and QTF Centre of Excellence, Department of Applied Physics, Aalto University School of Science, P.O. Box 15100, Aalto FI-00076, Finland*

(Received 16 October 2017; published 27 February 2018)

Making use of coherence and entanglement as metrological quantum resources allows us to improve the measurement precision from the shot-noise or quantum limit to the Heisenberg limit. Quantum metrology then relies on the availability of quantum engineered systems that involve controllable quantum degrees of freedom which are sensitive to the measured quantity. Sensors operating in the qubit mode and exploiting their coherence in a phase-sensitive measurement have been shown to approach the Heisenberg scaling in precision. Here, we show that this result can be further improved by operating the quantum sensor in the qudit mode, i.e., by exploiting d rather than two levels. Specifically, we describe the metrological algorithm for using a superconducting transmon device operating in a qutrit mode as a magnetometer. The algorithm is based on the base-3 semiquantum Fourier transformation and enhances the quantum theoretical performance of the sensor by a factor of 2. Even more, the practical gain of our qutrit implementation is found in a reduction of the number of iteration steps of the quantum Fourier transformation by the factor $\ln(2)/\ln(3) \approx 0.63$ compared to the qubit mode. We show that a two-tone capacitively coupled radio-frequency signal is sufficient for implementation of the algorithm.

DOI: 10.1103/PhysRevA.97.022115

I. INTRODUCTION

The idea of boosting metrological precision with the help of quantum resources has undergone impressive development during recent years [1,2]. Both types of quantum resources, coherence and entanglement, are used in either sequential or parallel strategies, respectively [3]. A key role in this endeavor is played by novel quantum algorithms, in particular, Kitaev's phase estimation [4,5] and the quantum Fourier transformation (QFT) and its semiclassical variant [6], both exploiting phase coherence as their quantum resource and thus following the sequential strategy. Previous theoretical and experimental work in this direction has all been rooted in a base-2 computational scheme that exploits qubits as measuring devices. In this paper, we demonstrate that a superconducting transmon device [7] operated in a qutrit (or base-3) mode offers an enhanced performance as a magnetic-field sensor; we present a specific algorithm exploiting the semiclassical quantum Fourier transform as well as the required radio-frequency (rf) voltage pulses for its implementation.

The use of entanglement-free protocols in metrology has been developed in several steps, first the problem of measuring the magnitude of classical fields was addressed [8], followed by a suggestion to quantify the mesoscopic magnetic field generated by an assembly of nuclear magnetic moments [9] and a proposal to use nitrogen–vacancy (NV) centers in diamond for nanoscale magnetometry [10]. The basic concept of this type of measurement was first used in the measurement of an optical phase through interferometry [11] and followed by the implementation of a high-dynamic-range magnetic-field sensor in the form of an NV center [12]. An alternative route has been taken by starting from the statistical counting of charges in mesoscopic transport [13], which requires inclusion of the measurement apparatus in the analysis. Originally, the latter was described by a spin that interacts with the charge-transporting lead within a Gedanken experiment. This idea was later developed into a realistic setup with a measurement device in the form of a charge or flux qubit [14,15]. Subsequently, statistical counting has been refined to an algorithm that counts the number of charges traversing the lead by making full use of quantum engineering ideas in combination with the semiclassical Fourier transform [16]. While all of the above work is based on qubits or base-2 counting, the concept of quantum counting [16] suggests a natural generalization of such a scheme to qudits or base-d counting [17]. Here, we propose an application of the qudit counting algorithm to a metrological measurement scheme for a magnetometer that makes use of a superconducting transmon device [7] operated in a qutrit mode. Making efficient use of the larger Hilbert space of a transmon qutrit and its specific linear energy level dependence on the measured magnetic flux then allows for faster acquisition of information and thereby more efficient measurement.

The algorithmic use of quantum engineered devices requires a nonlinear spectrum in order to address the quantum states individually. Superconducting circuit devices with Josephson junctions in loop geometries [18] can be viewed as artificial atoms; they exhibit energy spectra with unequal level spacings that can be designed on demand. Moreover, the position of energy levels in such devices is sensitive to the magnetic flux penetrating the SQUID loop of the artificial atom. In particular, the ultrahigh sensitivity of the transition frequency of the flux qubit [19] allows for its use as an ultrahighly sensitive magnetic

*lebedev@itp.phys.ethz.ch

flux sensor [20]. Unfortunately, the high sensitivity of flux qubits to low-frequency noise [21] reduces their coherence time, which makes them unfavorable for the implementation of quantum metrological procedures. On the other hand, the special design of the transmon atom [7] renders this device insensitive to the background charge noise, resulting in longer coherence times. Recently, Kitaev- and Fourier-like phase estimation algorithms have been successfully implemented in a dc magnetic-flux measurement with a transmon qubit [22], resulting in an algorithmically improved sensitivity in the high dynamic range.

The spectrum of a transmon atom is characterized by a particularly simple form that corresponds to a harmonic oscillator with a weak nonlinearity. Furthermore, the transmon atom's spectrum has a linear magnetic-flux dependence of the excited states with respect to the ground state (to leading order in the low ratio $E_{\rm C}/E_{\rm J}$ of the charge and Josephson energies of the transmon atom). Such a linear flux dependence allows one to exploit several excited levels of the transmon atom and implement a Fourier phase-estimation algorithm operating in the qudit regime. On the other hand, the charge degree of freedom enters the spectrum in a nonlinear way, allowing for the transmon's manipulation via capacitively coupled rf fields. Such coherent manipulation of a transmon atom operating in a qutrit regime has been demonstrated recently in several works [23,24]; below, we show how to exploit the combination of these features in the effective operation of the transmon as a magnetometer approaching Heisenberg scaling over the coherence time of the device.

Operating the transmon in the Heisenberg limit, i.e., attaining a measurement precision that scales in the invested resources R as $1/R$ rather than $1/\sqrt{R}$, requires a suitable metrological algorithm, in our case, the semiclassical Fourier transform. The basic step in this algorithm is a Ramsey cycle of duration τ that accumulates a phase $\phi = \mu H\tau/\hbar$ involving the magnetic field H to be measured; here, the magnetic moment μ plays the role of a coupling constant. Subsequent Ramsey cycles with incrementally reduced times τ, readout, and use of the result in the next step allow us to implement the quantum Fourier transformation, which boosts the device performance to make it attain the Heisenberg limit. This QFT is usually implemented in a binary system exploiting qubit devices. The implementation of this algorithm in a ternary system with qutrits improves the performance by a factor of 2, i.e., using half the resources, one arrives at the same precision as with the binary implementation. This information-theoretical result is further improved when considering the number of steps required for the same precision. Such a performance criterion makes sense, as most of the time required for the measurement is invested in the preparation and readout of the transmon, which has to be repeated at every step. It turns out that the number of steps is reduced by a factor of $\ln(2)/\ln(3) \approx 0.63$ when replacing the qubit mode with a qutrit implementation, a considerable speedup of the measurement.

In the following, we briefly recapitulate the binary metrological algorithm (Sec. II) and then extend the discussion to the ternary system, which exploits qutrits (Sec. III). The comparison between the two procedures in Sec. IV leads us to the performance results discussed above. In Sec. V, we discuss the spectral properties of the transmon device and find the specific rf pulses that prepare the qutrit for measurement and for readout: Essentially, these pulses generate a basis change (and back) from the computational basis (where the qutrit is operated) to the 'counting' or measurement basis, where the field imposes its characteristic 'rotation' of the qutrit that encodes the unknown magnitude of the field. It turns out that a two-tone pulse addressing the first and second excited states is sufficient to perform this task. In Sec. VI, we summarize and conclude our discussion.

II. QUBIT METROLOGICAL PROCEDURE

We start with a brief summary of the standard qubit-based metrological procedure for the measurement of a constant magnetic field. The elementary step in this measurement scheme is a Ramsey interference experiment where the qubit (or, equivalently, a spin-1/2) is prepared in an equally weighted (or balanced) superposition of its z-polarized states $|\downarrow\rangle$ and $|\uparrow\rangle$, $|\psi_0\rangle = (|\downarrow\rangle + |\uparrow\rangle)/\sqrt{2}$. The state $|\psi_0\rangle$ is located in the equatorial xy plane of the Bloch sphere and can be prepared by performing a $\pi/2$ rotation of the $|\downarrow\rangle$ state around a y axis, $|\psi_0\rangle = \hat{U}_y(\pi/2)|\downarrow\rangle$. Next, the state $|\psi_0\rangle$ is exposed during a time interval τ to a magnetic field H directed along the z axis, $|\psi_0\rangle \to \exp(-i\hat{\sigma}_z\phi/2)|\psi_0\rangle \equiv |\psi_\phi\rangle$, with $\phi = \mu H\tau/\hbar$ and μ the magnetic moment of the spin. As a result, the initial state $|\psi_0\rangle$ picks up the additional field-sensitive relative phase ϕ, $|\psi_\phi\rangle = (e^{-i\phi/2}|\downarrow\rangle + e^{i\phi/2}|\uparrow\rangle)/\sqrt{2}$. The last step in the Ramsey interference experiment is the readout procedure, where the information about the value of the magnetic field encoded in the qubit state is extracted through a projective measurement of the spin polarization along the z axis. In order to make the outcome probabilities $P_{\uparrow,\downarrow}$ depend on the magnetic field H, the state $|\psi_\phi\rangle$ is first transformed by applying a unitary readout operation, which coincides with that for the preparation in the qubit case, $|\psi_{\rm out}\rangle = \hat{U}_y(\pi/2)|\psi_\phi\rangle = -i\sin(\phi/2)|\downarrow\rangle + \cos(\phi/2)|\uparrow\rangle$. Repeating this Ramsey cycle several times, one can accumulate enough statistics and extract the value of the field H (see Refs. [15,17]).

Quite importantly, for the specific situation where the magnetic field H can assume only two values, $H = 0$ and $H = h$, one can unambiguously distinguish these two possibilities during a single Ramsey cycle, i.e., a single-shot measurement. Indeed, adjusting the time delay τ such that $\phi = \mu h\tau/\hbar = \pi$, one has that either $|\psi_\phi\rangle = |\psi_0\rangle$ or $|\psi_\phi\rangle = |\psi_1\rangle = (|\downarrow\rangle - |\uparrow\rangle)/\sqrt{2}$ and, hence, $|\psi_{\rm out}\rangle = |\uparrow\rangle$ or $|\psi_{\rm out}\rangle = |\downarrow\rangle$. This results in the probabilities $P_\uparrow = 1$ and $P_\downarrow = 0$ for $H = 0$ and $P_\uparrow = 0$ and $P_\downarrow = 1$ for $H = h$, allowing for a single-shot distinction between the two field values. The basis states $|\uparrow\rangle$ and $|\downarrow\rangle$ then define the so-called computational basis, while the states $|\psi_0\rangle$ and $|\psi_1\rangle$ form the counting basis.

The above remarkable fact can be further exploited to distinguish between 2^K discrete magnetic-field values with only K Ramsey experiments: Let the magnetic field $H \in [0, 2h_0]$ assume only discrete values that correspond to an exact K-bit fractional binary representation of the form

$$H = h_0\left(\frac{b_0}{2^0} + \frac{b_1}{2^1} + \frac{b_2}{2^2} + \cdots + \frac{b_{K-1}}{2^{K-1}}\right), \qquad (1)$$

where the amplitudes $b_n, n = 0, \ldots, K-1$, take binary values 0 and 1. Let us also choose an elementary time delay τ_0 such

that $\mu h_0 \tau_0/\hbar = \pi$. A Ramsey measurement with an enhanced time delay $\tau_{K-1} = 2^{K-1}\tau_0$ then accumulates a phase $\phi_{K-1} = \pi b_{K-1} + 2\pi n$, where the integer $n = 2^{K-1}b_0 + \cdots + 2b_{K-2}$ is given by the previous bits b_n, $n = 0, \ldots, K-2$. Although this first Ramsey experiment provides the phase ϕ_{K-1} only modulo 2π, the even or odd outcome for this modulo-2π phase allows for the unambiguous identification of the last binary digit b_{K-1}.

In the next step, the time delay in the Ramsey experiment is twice reduced, $\tau_{K-2} = 2^{K-2}\tau_0$. The accumulated field-sensitive phase is now given by $\phi_{K-2} = \pi(b_{K-2} + b_{K-1}/2) \mod 2\pi$. Since we have learned the value of the bit b_{K-1} in the previous measurement, we can apply an additional rotation, $\hat{U}_z(-\pi b_{K-1}/2)$, prior to the readout operation in order to compensate for the residual phase $\pi b_{K-1}/2$. The subsequent readout operation and measurement along z provide the next bit, b_{K-2}, in a deterministic way. Proceeding analogously with gradually decreased time delays $2^{K-3}\tau_0, 2^{K-4}\tau_0, \ldots, \tau_0$ allows for the unambiguous determination of all bits $b_{K-1}, b_{K-2}, \ldots, b_0$ in the binary representation of the magnetic field H and thus its precise selection out of the 2^K discrete allowed values [see Eq. (1)].

III. QUTRIT METROLOGY

Next, we consider the generalization of the above qubit-based metrological scheme to a qutrit, i.e., a quantum system that is endowed with a three-dimensional Hilbert space. Let the quantum system in question be a spin-1 system with (computational) basis states $|0\rangle$, $|1\rangle$, and $|2\rangle$ corresponding to the $m_z = -1, 0$, and 1 angular-momentum polarizations along the z axis. As in the qubit case, we prepare the qutrit in a *balanced* state, $|\psi_0\rangle = (|0\rangle + |1\rangle + |2\rangle)/\sqrt{3}$, and expose it to a constant magnetic field H directed along the z axis during the time τ. As a result, the information about the value of the field is encoded into the relative phases of the qutrit state,

$$|\psi_\phi\rangle = \frac{1}{\sqrt{3}}\left(|0\rangle + e^{i\phi}|1\rangle + e^{2i\phi}|2\rangle\right), \tag{2}$$

where $\phi = \mu H \tau/\hbar$ and we have omitted the overall phase factor $e^{-i\phi}$.

To start with, we consider a situation where the magnetic field assumes only one of three values, $H \in \{0, h, 2h\}$, $h > 0$; the task then is to unambiguously distinguish these three alternatives via a single-shot measurement of the state, (2); such a one-shot discrimination is indeed possible as shown in Ref. [17] within the context of the quantum counting problem. We expose the initial balanced state $|\psi_0\rangle$ during a specific time interval τ_0 to the field such that the phase $\phi = \mu h \tau_0/\hbar$ assumes the value $\phi = 2\pi/3$. As a result, the qutrit ends up in one of the counting states, $|\psi_\phi\rangle = |\psi_0\rangle$, $|\psi_\phi\rangle = |\psi_1\rangle = (|0\rangle + e^{2\pi i/3}|1\rangle + e^{-2\pi i/3}|2\rangle)/\sqrt{3}$, or $|\psi_\phi\rangle = |\psi_2\rangle = (|0\rangle + e^{-2\pi i/3}|1\rangle + e^{2\pi i/3}|2\rangle)/\sqrt{3}$, depending on the discrete field value, 0, h, or $2h$. Applying a base-d quantum inverse Fourier transformation, $\hat{F}_d^{-1}$,

$$\hat{F}_d^{-1}|n\rangle = \frac{1}{\sqrt{d}}\sum_{k=0}^{d-1} \mathrm{e}^{-2\pi i n k/d}\,|k\rangle, \tag{3}$$

with $d = 3$, to these counting states, one can check that the resulting state $|\psi_{\text{out}}\rangle = \hat{F}_3^{-1}|\psi_\phi\rangle$ coincides with one of the computational states, $|0\rangle$, $|1\rangle$, or $|2\rangle$, depending on the magnetic field H taking the value 0, h, or $2h$, respectively. Therefore, measuring the polarization of the resulting state $|\psi_{\text{out}}\rangle$ along the z axis allows for the unambiguous distinction between the three possible values of the magnetic field.

Next, consider the situation where the magnetic field H has an exact ternary representation

$$H = h_0\left(\frac{t_0}{3^0} + \frac{t_1}{3^1} + \cdots + \frac{t_{K-1}}{3^{K-1}}\right), \tag{4}$$

where the amplitudes (or trits) t_n, $n = 0, \ldots, K-1$, can take only three discrete values: 0, 1, and 2. Then, similarly to the qubit case, one can successively determine all K trinary digits starting from the least significant digit t_{K-1} within K separate preparation-exposure-readout steps. Indeed, in the first step, we prepare the qutrit in the balanced state $|\psi_0\rangle$ and expose it to the magnetic field H during the time interval $\tau_{K-1} = 3^{K-1}\tau_0$, where τ_0 is chosen to satisfy the relation $\mu h_0 \tau_0/\hbar = 2\pi/3$. Then the magnetic-field-dependent phase $\phi_{K-1} = (2\pi/3)\,t_{K-1} \mod 2\pi$ can only take the three values 0, $2\pi/3$, and $4\pi/3$, which can be unambiguously distinguished by the inverse Fourier transform in the readout step described above. Next, the digit t_{K-2} is determined by reducing the exposure time by one-third, $\tau_{K-2} = 3^{K-2}\,\tau_0$, which provides the field-dependent phase $\phi_{K-2} = (2\pi/3)(t_{K-2} + t_{K-1}/3)$. Making use of the digit t_{K-1} found in the previous step, the residual phase $2\pi t_{K-1}/9$ is compensated before readout through projection along z, which leads to the next trinary digit or trit t_{K-2}, and so on.

In the most general situation, the magnetic field H assumes continuous values and has no exact finite representation as in Eq. (1) or (4). Hence, the number of trinary (or binary) digits needed to describe it is infinite and one cannot measure the field H exactly with a finite number of preparation-exposure-readout steps. Still, we can find the approximate value of the field by detecting the first K digits of its numerical representation. For example, using a base-3 representation with qutrits and applying the magnetic field H during the time interval τ_{K-1} to the balanced state $|\psi_0\rangle$, the magnetic field induces the phase $\phi_{K-1} = (2\pi/3)t_{K-1} + 3^{K-1}\delta\phi$, where the residual phase $\delta\phi \in [0, \pi/3^K]$ as given by

$$\delta\phi = \frac{2\pi}{3}\left(\frac{t_K}{3^K} + \frac{t_{K+1}}{3^{K+1}} + \cdots\right) \tag{5}$$

is unknown and can no longer be compensated. As a consequence, rather than definitive outcomes, we have to find the probabilities P_k of observing the qutrit in the states $|k\rangle$, $k = 0, 1, 2$. Applying the inverse Fourier transform and analyzing the result, we find that the probabilities

$$\begin{aligned} P_0 &= \tfrac{1}{9}[1 + 2\cos(2\pi\, t_{K-1}/3 + 3^{K-1}\delta\phi)]^2, \\ P_1 &= \tfrac{1}{9}[1 + 2\cos(2\pi\,(t_{K-1} - 1)/3 + 3^{K-1}\delta\phi)]^2, \\ P_2 &= \tfrac{1}{9}[1 + 2\cos(2\pi\,(t_{K-1} - 2)/3 + 3^{K-1}\delta\phi)]^2 \end{aligned} \tag{6}$$

deviate from 0 and unity due to the unknown phase $\delta\phi$, hence, we can no longer distinguish different t_{K-1} values unambiguously. Instead, we must resort to a statistical analysis and select between the three alternatives $t_{K-1} = 0$, 1, and 2 by

finding the maximum probability P_k, $k = 0,1,2$. In practice, the weights of the three probabilities in Eq. (6) are disjoint and a single measurement is sufficient to determine the trit's value with good confidence; the overall success probabilities for the measurement schemes discussed below are calculated on the basis of this assumption. Repeating the procedure for the remaining $K-1$ trits including the required phase compensation prior to the readout, one arrives at a set of K trinary digits $\vec{t} \equiv t_0, \ldots, t_{K-1}$. The overall probability of observing the trinary string $\vec{t}$, given some unknown magnetic field H, is given by

$$P(\vec{t}\,|H) = \prod_{k=0}^{K-1} \frac{1}{9}\{1 + 2\cos[3^k(\phi(H) - \tilde{\phi}_{\vec{t}})]\}^2, \qquad (7)$$

where the phase $\tilde{\phi}_{\vec{t}} = (2\pi/3)\sum_{k=0}^{K-1} t_k/3^k$ relates to the string $\vec{t}$ and $\phi(H) = \mu H \tau_0/\hbar$ is the true field-induced phase; for the exact trinary value of H and its associated string $\vec{t}$, we have $P(\vec{t}\,|H) = 1$.

In the next step, we make use of Bayes' theorem and infer the probability $P(\phi(H)|\vec{t}\,)$ for the accumulated phase $\phi(H)$, provided we have observed a string $\vec{t}$, $P(\phi(H)|\vec{t}\,) \propto P(\vec{t}\,|H)$. Making use of the trigonometric identity $\sin(3\alpha) = \sin(\alpha)[3 - 4\sin^2(\alpha)]$, one finds that

$$P(\phi(H)|\vec{t}) = \frac{1}{2\pi}\frac{\sin^2[3^K(\phi(H) - \tilde{\phi}_{\vec{t}})/2]}{3^K \sin^2[(\phi(h) - \phi_{\vec{t}})/2]}. \qquad (8)$$

A similar analysis provides the result

$$P(\phi(H)|\vec{b}) = \frac{1}{2\pi}\frac{\sin^2[2^K(\phi(H) - \tilde{\phi}_{\vec{b}})/2]}{2^K \sin^2[(\phi(H) - \phi_{\vec{b}})/2]} \qquad (9)$$

for the qubit-based protocol, where $\vec{b}$ is the K-bit string learned during the K-step measurement process and $\tilde{\phi}_{\vec{b}} = \pi\sum_{k=0}^{K-1} b_k/2^k$.

The above qubit and qutrit Fourier metrological schemes can be generalized to a setup with qudits that are endowed with a d-dimensional Hilbert space. The qudit then is prepared in the balanced state $|\psi_0\rangle = (1/\sqrt{d})\sum_{j=0}^{d-1}|j\rangle$ and subsequently experiences a magnetic-phase accumulation, $|\psi_0\rangle \to |\psi_\phi\rangle = (1/\sqrt{d})\sum_{j=0}^{d-1} e^{ij\phi}|j\rangle$, followed by a d-base inverse Fourier readout measurement. The posterior probability density for the measured phase $\phi(H)$ is given by

$$P(\phi(H)|\vec{x}) = \frac{1}{2\pi}\frac{\sin^2[d^K(\phi(H) - \tilde{\phi}_{\vec{x}})/2]}{d^K \sin^2[(\phi(H) - \phi_{\vec{x}})/2]}, \qquad (10)$$

where $\vec{x}$ is a string of K base-d digits. Using the relation $\lim_{\gamma\to\infty}[\sin^2(\gamma x)/\pi\gamma x^2] = \delta(x)$ one easily checks that both results approach the limit of the δ function $P(\phi(H)|\vec{x}\,) \to \delta(\phi(H) - \tilde{\phi}_{\vec{x}})$ when $K \to \infty$.

Next, we discuss the impact of a false digit assignment on the measurement outcome of the Fourier metrological scheme. This follows from the probability density plot $P(\phi|\vec{x}\,) \equiv P(\delta\phi)$ evaluated as a function of the estimation error $\delta\phi = \phi - \tilde{\phi}_{\vec{x}}$, which is shown in Fig. 1 for the qubit- and qutrit-based algorithms.

Both plots show a sharp central peak, $\delta\phi \in [-2\pi/d^K, 2\pi/d^K]$, $d = 2$ or 3, and a number of decaying satellite peaks. These satellite peaks derive from the incorrect assignment of the binary b_i or trinary t_i digit during the measurement run. The first satellites correspond to the false assignment of the least significant digit in the first step of the procedure, while the far weaker satellites farther out correspond to assignment errors of subsequent readouts. This analysis shows that the Fourier metrological procedure is stable with respect to the assignment errors: the probability of determining a false digit decreases for each step in the procedure, resulting in a confidence level that is highest for the most significant digits and decreases for the measurement of the less significant digits. The probability that the observed value of the phase ϕ lies within the region of the central peak, and hence no error has been made in the assignment of digits, is given by

$$P\left(\delta\phi \in \left[-\frac{2\pi}{d^K}, \frac{2\pi}{d^K}\right]\right) \approx \frac{1}{\pi}\int_{-\pi}^{\pi} dy \frac{\sin^2 y}{y^2} \approx 0.903, \qquad (11)$$

where we have assumed a large K: the error probability saturates and does not depend on the number of steps K (or, equivalently, the number of digits), manifesting the stability of the Fourier procedure.

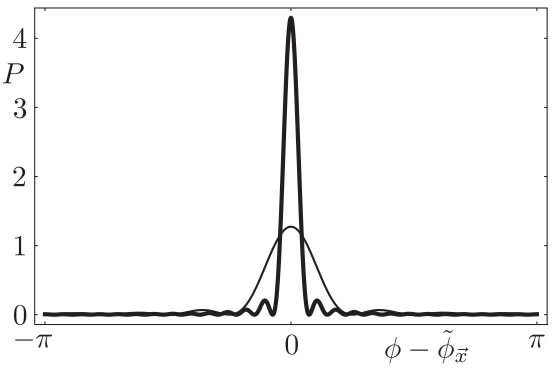

FIG. 1. Probability density plots $P(\phi - \tilde{\phi}_{\vec{x}})$ for the $K = 3$ step Fourier metrological procedure operated in the qutrit (thick line) and qubit (thin line) regimes.

IV. COMPARING THE QUBIT AND QUTRIT PROCEDURES

The posterior distribution functions for the phase $\phi(H)$ in the qutrit and qubit metrological procedures [see Eqs. (8) and (9)] allows us to compare the efficiencies of the two schemes quantitatively and reveal the advantage of using a higher-dimensional quantum system for metrological purposes. Let the unknown magnetic field H be located somewhere within the continuous interval $H \in [0, H_0]$. Then, as follows from Eqs. (1) and (4), the field scales for the qubit- and qutrit-based metrology are chosen as $h_0^{\rm qb} = H_0/2$ and $h_0^{\rm qt} = H_0/3$ and the corresponding minimal Ramsey delays are given by $\tau_0 = 2\pi\hbar/\mu H_0$. During the K steps, the qubit and qutrit metrological procedures learn about the magnetic field to a precision $(\delta H)_{\rm qb} = H_0/2^K$ and $(\delta H)_{\rm qt} = H_0/3^K$. These K-step precision boundaries have to be related to the amount of quantum resources required to achieve them. The quantum resource exploited in our metrological procedures is the coherence of the quantum devices, which can be quantified by the net coherence (or phase accumulation) time accumulated during the K steps [25]. For each of the two protocols, this

time is given by

$$T_{\rm qb} = \tau_0 \sum_{k=0}^{K-1} 2^k \approx \frac{2\pi\hbar}{\mu H_0}\, 2^K, \tag{12}$$

$$T_{\rm qt} = \tau_0 \sum_{k=0}^{K-1} 3^k \approx \frac{2\pi\hbar}{\mu H_0}\, \frac{3^K}{2}. \tag{13}$$

Expressing the K-step precisions δH through the net coherence time,

$$(\delta H)_{\rm qb} = \frac{2\pi\hbar}{\mu}\,\frac{1}{T_{\rm qb}}, \quad (\delta H)_{\rm qt} = \frac{\pi\hbar}{\mu}\,\frac{1}{T_{\rm qt}}, \tag{14}$$

one notes that both procedures attain the Heisenberg limit, with the precision δH scaling as the inverse of the total coherence time, but the qutrit procedure has a twice better prefactor. For the general qudit metrological scheme, the combination of $(\delta H)_{\rm qd} = H_0/d^K$, $T_{\rm qd} = \tau_0 d^K/(d-1)$, and $\tau_0 = 2\pi\hbar/\mu H_0$ produces the sensitivity,

$$(\delta H)_{\rm qd} = \frac{2\pi\hbar}{\mu}\,\frac{1}{(d-1)T_{\rm qd}}. \tag{15}$$

In practice, however, the phase accumulation time is the minimal time used in a Ramsey experiment. Most of the overall measurement time is spent on the measurement and reinitialization of the quantum devices. Hence, in practice, the speed of the metrological procedure is mostly defined by the number K of steps required to achieve a given precision. Here, the qutrit-based procedure has a clear advantage: in order to achieve a relative precision $\delta H/H_0$ it requires approximately $K \sim -\log_3(\delta H/H_0)$ steps, that is, $\ln(2)/\ln(3) \approx 0.63$ fewer than the number of steps $K \sim -\log_2(\delta H/H_0)$ needed for the qubit-based scheme.

V. METROLOGY WITH A TRANSMON DEVICE

The working principle of a transmon qubit as a magnetic-flux sensor has been recently demonstrated in Ref. [22]; here, we describe how the qutrit metrological protocol can be realized with a transmon device. The superconducting transmon [7] involves a capacitively shunted SQUID loop and constitutes an excellent candidate to implement qudit metrological algorithms. Its dynamics is described by the Hamiltonian

$$\hat{H} = 4E_{\rm c}(\hat{n} - n_g)^2 - E_{\rm J}(\Phi)\cos(\hat{\varphi}), \tag{16}$$

where $\hat{n}$ is the number of Cooper pairs transmitted between superconducting islands with a charging energy $E_{\rm c}$ and relative phase $\hat{\varphi}$ and n_g is the charge bias. The Josephson energy $E_{\rm J}(\Phi)$ of the SQUID loop depends on the flux Φ through the loop,

$$E_{\rm J}(\Phi) = E_{\rm J\Sigma}\sqrt{\cos^2(\pi\Phi/\Phi_0) + a^2\sin^2(\pi\Phi/\Phi_0)}. \tag{17}$$

Here, $E_{\rm J\Sigma} = E_{\rm J1} + E_{\rm J2}$ is the total energy of the two Josephson junctions in the SQUID loop, $a = (E_{\rm J1} - E_{\rm J2})/E_{\rm J\Sigma}$ is the junctions' asymmetry, and Φ_0 is the magnetic flux quantum.

The transmon atom is operated in the limit where $E_{\rm J}/E_{\rm c} \sim 80-200$. Its energy spectrum comprises a discrete set of nonequidistant energy levels with positions that depend on the magnetic flux Φ penetrating the SQUID loop of the device. Expanding the $\cos(\hat{\varphi})$ term in the Hamiltonian, Eq. (16), and treating the term quartic in $\hat{\varphi}$ as a perturbation, we obtain (to leading order) the transmon's energy spectrum in the form

$$E_n \approx \sqrt{8E_{\rm c}E_{\rm J}(\Phi)}\left(n+\frac{1}{2}\right) - E_{\rm J}(\Phi) - \frac{E_{\rm c}}{12}(6n^2+6n+3), \tag{18}$$

The nonlinearity of the spectrum $E_{n+1} - E_n = -E_{\rm c}(n+1) + \sqrt{8E_{\rm c}E_{\rm J}(\Phi)}$ allows for the individual addressing of the transmon's quantum states through application of pulses of electromagnetic radiation with specific frequencies. On the other hand, to leading order, the dependence of the spectrum on the magnetic flux Φ is linear in n; while second-order corrections $\propto E_{\rm c}(E_{\rm J}/E_{\rm c})^{-1/2}$ do modify this result, these corrections are small and we neglect them in the following.

In order to manipulate the first two excited states of our transmon atom, we consider a two-tone rf pulse that generates a time-varying electric potential difference of the form

$$V(t) = \Omega(t)(V_1\cos(\omega_1 t) + V_2\cos(\omega_2 t)) \tag{19}$$

at the transmon's capacitor, where $\Omega(t)$ is the pulse envelope and $V_{1(2)}$ are the amplitudes of the pulse components with tone frequencies $\omega_{1(2)}$. The transmon evolution under the pulse $V(t)$ then is described by the Hamiltonian

$$\hat{H} = \sum_{n=0}^{\infty} E_n|n\rangle\langle n| + (\hbar g_{n,n+1}(t)|n\rangle\langle n+1| + \text{H.c.}), \tag{20}$$

with the transition amplitudes $\hbar g_{n,n+1}(t) = 2\beta eV(t)\,\langle n|\hat{N}|n+1\rangle$; here, $\hat{N}$ is the number operator of Cooper pairs transferred between the transmon's capacitor plates and β is a geometrical factor which quantifies the coupling between the transmon's capacitor and the rf field (see Ref. [7]).

Let the tone frequencies ω_1 and ω_2 be near the transition frequencies $\omega_{01} = (E_1 - E_0)/\hbar$ and $\omega_{12} = (E_2 - E_1)/\hbar$ of the first two pairs of levels, such that only the three lowest energy levels are affected by the rf field. We work in the rotating frame (or interaction representation) with respect to the 'free' Hamiltonian $\hat{H}_0 = \hbar\omega_1|1\rangle\langle 1| + \hbar(\omega_1+\omega_2)|2\rangle\langle 2|$. A quantum state of this effective three-level system can be represented as $|\Psi(t)\rangle = a_0(t)|0\rangle + a_1(t)|1\rangle + a_2(t)|2\rangle$. The time-dependent amplitudes $\vec{a}(t) = [a_0(t), a_1(t), a_2(t)]$ obey the Schrödinger equation $i\hbar\partial_t\vec{a}(t) = \hat{H}(t)\vec{a}(t)$, with the Hamiltonian assuming the following form in the rotating-wave approximation:

$$\hat{H}(t) = \hbar\begin{bmatrix} 0 & \Omega(t)\Delta_1 & 0 \\ \Omega(t)\Delta_1 & \omega_{01}-\omega_1 & \Omega(t)\Delta_2 \\ 0 & \Omega(t)\Delta_2 & \omega_{01}+\omega_{12}-\omega_1-\omega_2 \end{bmatrix}, \tag{21}$$

where $\Delta_1 = \beta eV_1\langle 0|\hat{N}|1\rangle/\hbar$ and $\Delta_2 = \beta eV_2\langle 1|\hat{N}|2\rangle/\hbar$ are effective transition amplitudes.

A. Qutrit metrological protocol

Our qutrit metrological scheme involves three steps that have to be implemented with the help of proper manipulation signals $V(t)$. In the first step, we prepare the transmon in a

balanced superposition of the form

$$|\Psi_0\rangle = \frac{1}{\sqrt{3}}(e^{i\varphi_0}|0\rangle + e^{i\varphi_1}|1\rangle + e^{i\varphi_2}|2\rangle) \equiv \frac{1}{\sqrt{3}}\begin{bmatrix} e^{i\varphi_1} \\ e^{i\varphi_2} \\ e^{i\varphi_3} \end{bmatrix}. \quad (22)$$

In the second step, the free evolution $\hat{U}(\Phi)$ of the transmon generates the additional phase factors $|1\rangle \to e^{i\phi}|1\rangle$ and $|2\rangle \to e^{i\phi'}|2\rangle$ with $\phi = [\omega_{01}(\Phi) - \omega_1]\tau$ and $\phi' = [\omega_{01}(\Phi) + \omega_{12}(\Phi) - \omega_1 - \omega_2]\tau$. The remarkable property of the transmon is that its level separations scale equally in magnetic flux [see Eq. (18)]. Starting from the reference magnetic flux Φ_c, we set the frequencies $\omega_1 = \omega_{01}(\Phi_c)$ and $\omega_2 = \omega_{12}(\Phi_c)$. Then $\phi' = 2\phi \equiv 2[\omega_{01}(\Phi) - \omega_{01}(\Phi_c)]\tau$ and the state $|\Psi_0\rangle$ evolves to the new balanced state

$$|\Psi_\phi\rangle = \frac{1}{\sqrt{3}}\begin{bmatrix} e^{i\varphi_0} \\ e^{i\varphi_1 + i\phi} \\ e^{i\varphi_2 + 2i\phi} \end{bmatrix}. \quad (23)$$

Finally, in the third step of our qutrit metrological procedure, we need to construct a unitary readout operator of the form

$$\hat{U}_r = \frac{1}{\sqrt{3}}\begin{bmatrix} e^{i\chi_0} & 0 & 0 \\ 0 & e^{i\chi_1} & 0 \\ 0 & 0 & e^{i\chi_2} \end{bmatrix}\begin{bmatrix} 1 & 1 & 1 \\ 1 & e^{-2\pi i/3} & e^{+2\pi i/3} \\ 1 & e^{2\pi i/3} & e^{-2\pi i/3} \end{bmatrix} \times \begin{bmatrix} e^{-i\varphi_0} & 0 & 0 \\ 0 & e^{-i\varphi_1} & 0 \\ 0 & 0 & e^{-i\varphi_2} \end{bmatrix}, \quad (24)$$

which represents a generalized base-3 inverse Fourier transform.

For the specific situation where the accumulated phase ϕ can only assume the three values 0, $2\pi/3$, and $4\pi/3 \leftrightarrow -2\pi/3$, this measurement scheme is deterministic and the transmon will always be found in one of the pure states $|0\rangle$, $|1\rangle$, or $|2\rangle$. Indeed, for $\phi = 2\pi/3$ or $\phi = 4\pi/3$, the state $|\Psi_0\rangle$ transforms into states

$$|\Psi_1\rangle = \frac{1}{\sqrt{3}}\begin{bmatrix} e^{i\varphi_0} \\ e^{i\varphi_1 + i\frac{2\pi}{3}} \\ e^{i\varphi_2 + i\frac{4\pi}{3}} \end{bmatrix}, \quad |\Psi_2\rangle = \frac{1}{\sqrt{3}}\begin{bmatrix} e^{i\varphi_0} \\ e^{i\varphi_1 + i\frac{4\pi}{3}} \\ e^{i\varphi_2 + i\frac{2\pi}{3}} \end{bmatrix}, \quad (25)$$

which together with $|\Psi_0\rangle$ form the (orthonormal) computational basis. Then the readout operation $\hat{U}_r$ provides a deterministic outcome,

$$\hat{U}_r|\Psi_j\rangle = e^{i\chi_j}|j\rangle, \quad j = 0,1,2. \quad (26)$$

For an arbitrary accumulated phase, the scheme is probabilistic and provides the probabilities

$$P_j(\phi) = |\langle j|\hat{U}_r\hat{U}(\Phi)\hat{U}_p|0\rangle|^2 = \tfrac{1}{9}[1 + 2\cos(\phi(\Phi) - 2\pi\, j/3)]^2, \quad j = 0,1,2, \quad (27)$$

of observing the transmon in state $|j\rangle$. The possible phase values ϕ then are divided into the three sectors $S_0 = [-\pi/3,\pi/3]$, $S_1 = [\pi/3,\pi]$, and $S_2 = [\pi,5\pi/3]$ with the maximal probability P_j indicating that $\phi \in S_j$.

B. Radio-frequency pulses for the metrological protocol

In order to implement our metrological protocol, we have to find appropriate rf pulses $V_p(t)$ and $V_r(t)$ that prepare the transmon in a balanced state and read out the state after its free evolution in the magnetic field to be measured. It turns out to be convenient to reverse the order and find the readout pulse first.

Hence, our next goal is to find an rf pulse $V_r(t)$ that generates a unitary readout operation of the form (24), a task that we tackle in three steps: (i) We show that any 3×3 unitary with equal-modulus matrix elements $|\hat{U}_{ij}| = 1/\sqrt{3}$ is of the form either $\hat{U}_r$ or $\hat{U}_r^{-1}$. (ii) We find the unitary associated with a rectangular two-tone rf pulse of finite duration τ_p. (iii) We determine the constraints on the rf pulse required for the readout action.

Starting with (i), we consider an arbitrary 3×3 unitary matrix $\hat{U}$ with all matrix elements of modulus $1/\sqrt{3}$. After multiplication with suitable diagonal phase matrices from the left and right, we can arrive at the form

$$\hat{U} \to \hat{U}' = \frac{1}{\sqrt{3}}\begin{bmatrix} 1 & 1 & 1 \\ 1 & e^{i\alpha_1} & e^{i\beta_1} \\ 1 & e^{i\alpha_2} & e^{i\beta_2} \end{bmatrix}, \quad (28)$$

where the remaining four phases have to satisfy the orthogonality constraints between columns, $1 + e^{i\alpha_1} + e^{i\alpha_2} = 0$, $1 + e^{i\beta_1} + e^{i\beta_2} = 0$, and $1 + e^{i(\alpha_1 - \beta_1)} + e^{i(\alpha_2 - \beta_2)} = 0$. It follows that the solutions of these constraints define either the Fourier transform $\hat{U}' = \hat{F}_3$ or its inverse $\hat{U}' = \hat{F}_3^{-1}$ [see Eq. (3)], which proves our statement.

Next, in step (ii), we consider a two-tone rf pulse with a rectangular shape of duration τ_p and frequencies $\omega_1 = \omega_{01}(\Phi_c) - 2\delta\omega$ and $\omega_2 = \omega_{12}(\Phi_c) + 2\delta\omega$. Such a pulse generates a unitary rotation of the qutrit $\hat{U} = \exp(-i\hat{H}\tau_p/\hbar) \equiv \exp(-i\hat{K})$, where

$$\hat{K} = \begin{bmatrix} 0 & \Delta_1 & 0 \\ \Delta_1 & 2\epsilon & \Delta_2 \\ 0 & \Delta_2 & 0 \end{bmatrix}, \quad \epsilon = \delta\omega\,\tau_p, \quad (29)$$

and $\Delta_{1,2}$ are effective transition amplitudes [see Eq. (21)]. The resulting unitary transformation has the form

$$\hat{U} = \begin{bmatrix} \frac{\Delta_2^2}{\Delta_1^2+\Delta_2^2} & 0 & -\frac{\Delta_1\Delta_2}{\Delta_1^2+\Delta_2^2} \\ 0 & 0 & 0 \\ -\frac{\Delta_1\Delta_2}{\Delta_1^2+\Delta_2^2} & 0 & \frac{\Delta_1^2}{\Delta_1^2+\Delta_2^2} \end{bmatrix} + e^{-i\epsilon}\cos(\xi)\begin{bmatrix} \frac{\Delta_1^2}{\Delta_1^2+\Delta_2^2} & 0 & \frac{\Delta_1\Delta_2}{\Delta_1^2+\Delta_2^2} \\ 0 & 1 & 0 \\ \frac{\Delta_1\Delta_2}{\Delta_1^2+\Delta_2^2} & 0 & \frac{\Delta_2^2}{\Delta_1^2+\Delta_2^2} \end{bmatrix} + \frac{ie^{-i\epsilon}\sin(\xi)}{\xi}\begin{bmatrix} \frac{\epsilon\Delta_1^2}{\Delta_1^2+\Delta_2^2} & -\Delta_1 & \frac{\epsilon\Delta_1\Delta_2}{\Delta_1^2+\Delta_2^2} \\ -\Delta_1 & -\epsilon & -\Delta_2 \\ \frac{\epsilon\Delta_1\Delta_2}{\Delta_1^2+\Delta_2^2} & -\Delta_2 & \frac{\epsilon\Delta_2^2}{\Delta_1^2+\Delta_2^2} \end{bmatrix}, \quad (30)$$

where $\xi = \sqrt{\epsilon^2 + \Delta_1^2 + \Delta_2^2}$.

Let us then, (iii), determine the parameters that generate the readout matrix $\hat{U}_r$. Following (i), we have to require that

$|[U_r]_{ij}|^2 = 1/3$. The conditions $|U_{12}|^2 = |U_{21}|^2 = 1/3$ and $|U_{23}|^2 = |U_{32}|^2 = 1/3$ imply that

$$\frac{\sin^2(\xi)}{\xi^2}\,\Delta_1^2 = \frac{1}{3}, \quad \frac{\sin^2(\xi)}{\xi^2}\,\Delta_2^2 = \frac{1}{3}, \tag{31}$$

which gives $\Delta_1^2 = \Delta_2^2 \equiv \Delta^2$. Accounting for the remaining conditions $|U_{11}|^2 = |U_{13}|^2 = 1/3$ and using the relation $2\Delta^2 = \xi^2 - \epsilon^2$, we arrive at the following system of transcendental equations:

$$\epsilon^2 = \xi^2\left(1 - \frac{2}{3\sin^2(\xi)}\right), \tag{32}$$

$$\cos(\epsilon)\cos(\xi) + \frac{\epsilon}{\xi}\sin(\epsilon)\sin(\xi) = 0. \tag{33}$$

Among its solutions, we choose the one with the minimal ϵ, as it corresponds to the shortest rf pulse for a given detuning $\delta\omega$, and find the numerical values $\epsilon_0 \approx 0.8525$, $\xi_0 \approx 2.0205$, and hence $\Delta_0 \approx 1.2953$. We note that the system of Eqs. (32) and (33) remains unchanged under a sign change of the parameters ϵ, Δ_1, and Δ_2 characterizing the Hamiltonian.

Let us consider the specific solution with $\epsilon = -\epsilon_0$ and $\Delta_1 = \Delta_2 = \Delta_0$. The corresponding pulse then generates the readout unitary transformation

$$\begin{aligned}\hat{U}_r &= \frac{1}{\sqrt{3}}\begin{bmatrix} e^{-i\frac{\pi}{6}} & -ie^{i\epsilon_0} & e^{-i\frac{5\pi}{6}} \\ -ie^{i\epsilon_0} & ie^{i2\epsilon_0} & -ie^{i\epsilon_0} \\ e^{-i\frac{5\pi}{6}} & -ie^{i\epsilon_0} & e^{-i\frac{\pi}{6}} \end{bmatrix} \\ &\equiv \begin{bmatrix} 1 & 0 & 0 \\ 0 & e^{i\epsilon_0 + i\frac{5\pi}{6}} & 0 \\ 0 & 0 & e^{i\frac{4\pi}{3}} \end{bmatrix} \hat{F}_3^{-1} \begin{bmatrix} e^{-i\frac{\pi}{6}} & 0 & 0 \\ 0 & -ie^{i\epsilon_0} & 0 \\ 0 & 0 & e^{-i\frac{5\pi}{6}} \end{bmatrix},\end{aligned} \tag{34}$$

which provides the desired inverse generalized Fourier transform.

As a preparation operator $\hat{U}_p$, we choose a unitary rotation generated by an rf pulse with $\epsilon = +\epsilon_0$ and $\Delta_1 = \Delta_2 = -\Delta_0$; i.e., the preparation pulse generates the inverse of the readout operator, $\hat{U}_p = \hat{U}_r^\dagger$.

The sign change in ϵ is trivially realized by inverting the detuning $\delta\omega \to -\delta\omega$. In order to change the sign (or, more generally, the phase) of the effective transition amplitudes $\Delta_{1,2}$, one can proceed with an appropriate modulation of the voltage signal $V(t)$. Making use of a standard IQ (in-phase and quadrature) mixing scheme, an incoming high-frequency signal $\cos(\omega_{\text{LO}}t)$ with the (local oscillator) frequency $\omega_{\text{LO}} = \frac{1}{2}[\omega_{01}(\Phi_c) + \omega_{12}(\Phi_c)]$ is first physically split (and partly phase shifted) into two separate signals, $\cos(\omega_{\text{LO}}t) \to \frac{1}{2}[\cos(\omega_{\text{LO}}t) + \sin(\omega_{\text{LO}}t)]$. These are independently mixed with the intermediate-frequency signals $A_1\Omega(t)\cos(\omega_{\text{IF}}t + \varphi)$ and $A_2\Omega(t)\sin(\omega_{\text{IF}}t + \varphi)$ generated by an arbitrary-waveform generator. Finally, the signals are recombined and the resulting output signal sent to the transmon is given by

$$\begin{aligned}V(t) = \frac{\Omega(t)}{4}&[(A_1 - A_2)\cos[(\omega_{\text{LO}} + \omega_{\text{IF}})t + \varphi] \\ &+ (A_1 + A_2)\cos[(\omega_{\text{LO}} - \omega_{\text{IF}})t - \varphi]].\end{aligned} \tag{35}$$

Choosing amplitudes $A_1 = 2(V_1 + V_2)$ and $A_2 = 2(V_2 - V_1)$, frequency $\omega_{\text{IF}} = \frac{1}{2}[\omega_{01}(\Phi_c) - \omega_{12}(\Phi_c)] - 2\delta\omega$, and phase $\varphi = 0$, one can generate the readout pulse. On the other hand, choosing the frequency $\omega_{\text{IF}} = \frac{1}{2}[\omega_{01}(\Phi_c) - \omega_{12}(\Phi_c)] + 2\delta\omega$ and the phase $\varphi = \pi$ together with the sign inversion of the detuning $\delta\omega$ reverses the sign of all three parameters ϵ, Δ_1, and Δ_2 and hence produces the preparation pulse.

C. Optimizing the transmon sensitivity

As follows from Eq. (15), the measurement precision that can be attained by the qudit metrological protocol depends on two factors, the magnetic moment μ of the transmon device and the longest phase coherence time $d^{K-1}\tau_0$ required for the longest run of the metrological protocol. The magnetic moment of the transmon can be obtained via the curvature of its transition frequency,

$$\mu = \hbar A\frac{\partial\omega_{01}(\Phi_c)}{\partial\Phi}, \tag{36}$$

where A is the area of the SQUID loop. Indeed, the relative phase $\phi = [\omega_{01}(\Phi) - \omega_{01}(\Phi_c)]\tau$ accumulated by the transmon's wave function is given by

$$\phi \approx \tau\frac{\partial\omega_{01}(\Phi_c)}{\partial\Phi}(\Phi - \Phi_c) = \frac{\mu\delta H\tau}{\hbar}, \tag{37}$$

where $\delta H = H - H_c$ is the magnetic field measured relative to the reference magnetic field H_c, $\Phi_c = AH_c$. In order to attain a better sensitivity, one has to deviate from the 'sweet spot,' the upper maximum of the transmon spectrum $\omega_{01}(\Phi)$ where $\mu = 0$, and take the device to a (locally) linear regime with a lower transition frequency. In the limit of an almost-symmetric Josephson junction loop with $a \to 0$, the maximal value of the transmon's magnetic moment is given by [see Eqs. (18) and (17)]

$$\mu = \pi\frac{A}{\Phi_0}\sqrt{\frac{8E_cE_{J\Sigma}}{a}}, \tag{38}$$

which occurs near the bottom of the transmon spectrum where $\tan^2(\pi\Phi_c/\Phi_0) = 1/a$. The result, Eq. (38), applies to the transmon limit $E_J \gg E_c$; for a symmetric device $a \to 0$, the largest moment μ appears near the point of maximal frustration $\Phi_c = \Phi_0/2$ where E_J becomes small and the approximation breaks down.

In our discussion above, we have implicitly assumed that the entire preparation–phase accumulation–readout sequence involves a total time that is much below the coherence (T_2) and relaxation (T_1) times of the transmon device. In a realistic situation, when operating the transmon away from the sweet spot the T_2 time is reduced and so is the number K of available steps for the metrological procedure. For a given qudit coherence time T_2, the delay time of the longest Ramsey sequence cannot exceed the T_2 time. Hence, the maximum number of steps in the Fourier procedure is limited by the condition $\tau_0 d^{K-1} = T_2$, which gives $K = 1 + \log_d(T_2/\tau_0)$ steps, where τ_0 is the minimum duration of a Ramsey sequence. Thus, the total amount of coherence time spent for the signal sensing is given by $T_{\text{qd}} = \tau_0\sum_{k=0}^{K-1} d^k = \tau_0(d^{K-1} - 1)/(d-1) \approx [d/(d-1)]T_2$ for $K \gg 1$. Then, according to Eq. (15), the best attainable field resolution can be estimated

as

$$[\delta H]_{T_2} \approx \frac{2\pi\hbar}{\mu\, d\, T_2}. \tag{39}$$

Hence, we have to optimize the product $\mu(\Phi_c)T_2(\Phi_c)$ for the best flux bias Φ_c, compromising between two opposing trends, the magnetic moment $\mu(\Phi_c)$ increasing and the coherence time $T_2(\Phi_c)$ decreasing away from the sweet spot. The magnetic moment of a transmon atom can attain a value of $10^5\mu_B$ (see Ref. [22]). Assuming a coherence time $T_2 \sim 1$ μs, one can estimate that a magnetic-field precision of order $\delta H \sim 0.1$ nT can be achieved.

A further improvement of the field resolution is possible only within a standard statistical measurement scheme [26] by repeating the longest Ramsey measurement with $\tau \sim T_2$ a large number, $N \gg 1$, of times. This leads to a standard scaling of the further field resolution with time duration t of the experiment: with $N = t/T_2$ we obtain a precision

$$[\delta H]_{t\gg T_2} \approx \frac{2\pi\hbar}{\mu\, d\, T_2\sqrt{t/T_2}} = \frac{2\pi\hbar}{\mu\, d\,\sqrt{T_2 t}}. \tag{40}$$

Therefore, the Heisenberg scaling is limited to measurement times shorter then the coherence time T_2 of the device, with the standard quantum limit restored for larger measurement times. The standard scaling, Eq. (40), can be achieved by a conventional scheme where one always measures the transmon state at the longest possible delay T_2 of the Ramsey sequence. However, such a conventional scheme has a limited measurement range ΔH for the field H that results from the 2π periodicity of the accumulated phase $\phi \sim \mu\Delta H T_2/\hbar$, i.e., $\Delta H \sim 2\pi\hbar/\mu T_2$. In contrast, the quantum procedure does not suffer from this limitation: its measurement range is defined only by the minimal time duration τ_0 of the Ramsey sequence, which is limited in practice by the time duration of the controlling rf pulses.

Making use of the above ideas in an experiment, a further practical restriction has to be considered besides the finite coherence time of the transmon device. First, the total duration of the experiment has to include the additional time spent for the measurement and reset of the transmon state. In fact, in the sensing experiment in Ref. [22] using the transmon qubit mode, most of the time of a single Ramsey measurement $T_{\rm rep}$ has been spent on the measurement and reset of the qubit $T_{\rm rep} \gg T_2$. In this limit, the long-time sensitivity of the sensor is reduced and given by

$$[\delta H]_{t\gg T_{\rm rep}\gg T_2} \approx \frac{2\pi\hbar}{\mu\, d\, T_2\,\sqrt{t/T_{\rm rep}}}. \tag{41}$$

Second, the higher-excited states of the transmon have larger dipole matrix elements and hence are more sensitive to the external electromagnetic environment [7]. Therefore, a transmon atom has specific T_1 and T_2 times for each excited state and the number of levels which can be used is naturally limited by the coherence time of the highest-energy state involved. In practice, one can start the Fourier metrological procedure in a qubit measurement mode at Ramsey delays corresponding to the largest T_2 time belonging to the first excited level and then continue in a qutrit mode when the Ramsey delays have dropped below the T_2 time of the second excited level. Finally, operating a transmon atom in a qudit regime requires a more involved characterization of its spectrum and calibration of the corresponding rf control pulses. At the same time, operating a transmon in the qutrit regime is a well-established experimental procedure [23,24], which motivates work directed at the experimental implementation of our qutrit metrological procedure.

VI. SUMMARY AND CONCLUSION

We have presented a variant of the standard quantum Fourier metrological procedure that replaces the usual qubit elements with qutrits and, more generally, with qudits. While all of these algorithms exploit phase coherence as their quantum resource, allowing them to reach the Heisenberg precision scaling, the use of higher-dimensional Hilbert spaces in the qutrit and qudit versions improves the prefactor of this scaling. Even more, going to qudit devices reduces the number of iteration steps in the Fourier procedure, thus providing a marked improvement in the measurement algorithm. As a specific example, we have discussed the use of a superconducting transmon device operated in the qutrit mode, which serves as an ideal resource for the measurement of dc and low-frequency magnetic fields, a consequence of the linear field dependence of the transmon's spectrum. It turns out, that a simple two-tone rf voltage signal in combination with a standard IQ mixing scheme suffices to produce the appropriate preparation and readout pulses for the Fourier metrological algorithm.

The scheme presented in this paper relies on the assumption that the longest measurement providing the least relevant but precision-limiting digit can be performed within the coherence or T_2 time of the transmon device; a further increase in precision proceeds via a conventional measurement procedure and follows the standard (shot-noise- or quantum-limited) scaling in precision. Furthermore, given a finite coherence time T_2, the algorithm can be further optimized to deal with this situation: Besides properly tuning the qutrit's reference flux or working point Φ_c as discussed above, other elements of the algorithm can be improved: e.g., a finite T_2 time may require more than a single Ramsey measurement at each time delay τ_k, $k = 1, \ldots K$, which modifies the probability, Eq. (10), of arriving at the correct sequence $\vec{x}$ of digits. In addition, the time delays τ_k appearing in the metrological protocol are subject to optimization, i.e., they must be chosen differently from the ideal case. The situation with finite T_1 and T_2 times then requires a separate study that will be the topic of a future analysis.

ACKNOWLEDGMENTS

We acknowledge discussions with Pertti Hakonen and Vladimir Manucharyan. The research was supported by Government of the Russian Federation Agreement 05.Y09.21.0018,RFBR Grant Nos. 17- 02-00396A and 18-02-00642A, the Foundation for the Advancement of Theoretical Physics 'BASIS', the Ministry of Education and Science of the Russian Federation Grant No. 16.7162.2017/8.9 (A.V.L., A.R.S., and V.V.Z. in part related to Section IV), the Swiss National Foundation via the National Centre of Competence in Research in Quantum Science and Technology (NCCR QSIT), the Pauli Center for Theoretical Physics, Academy of Finland Centers of Excellence, "Low Temperature

Quantum Phenomena and Devices" (Project No. 250280) and "Quantum Technology Finland (QTF)" (Project No. 312296), and the Center for Quantum Engineering at Aalto University. V.Z. and A.S. acknowledge support from the 5-top 100 program via the Laboratory of Quantum Information Theory (MIPT).

[1] V. Giovannetti, S. Lloyd, and L. Maccone, Nat. Photon. **5**, 222 (2011).
[2] C. L. Degen, F. Reinhard, and P. Cappellaro, Rev. Mod. Phys. **89**, 035002 (2017).
[3] V. Giovannetti, S. Lloyd, and L. Maccone, Phys. Rev. Lett. **96**, 010401 (2006).
[4] A. Yu. Kitaev, arXiv:quant-ph/9511026.
[5] R. Cleve, A. Ekert, C. Macchiavello, and M. Mosca, Proc. R. Soc. Lond. A **454**, 339 (1998).
[6] R. B. Griffiths and C.-S. Niu, Phys. Rev. Lett. **76**, 3228 (1996).
[7] J. Koch, T. M. Yu, J. Gambetta, A. A. Houck, D. I. Schuster, J. Majer, A. Blais, M. H. Devoret, S. M. Girvin, and R. J. Schoelkopf, Phys. Rev. A **76**, 042319 (2007).
[8] L. Vaidman and Z. Mitrani, Phys. Rev. Lett. **92**, 217902 (2004).
[9] G. Giedke, J. M. Taylor, D. D'Alessandro, M. D. Lukin, and A. Imamoglu, Phys. Rev. A **74**, 032316 (2006).
[10] R. S. Said, D. W. Berry, and J. Twamley, Phys. Rev. B **83**, 125410 (2011).
[11] B. L. Higgins, D. W. Berry, S. D. Bartlett, H. M. Wiseman, and G. J. Pryde, Nature **450**, 393 (2007).
[12] G. Waldherr, J. Beck, P. Neumann, R. S. Said, M. Nitsche, M. L. Markham, D. J. Twitchen, J. Twamley, F. Jelezko, and J. Wrachtrup, Nat. Nanotechnol. **7**, 105 (2012).
[13] L. S. Levitov, H. W. Lee, and G. B. Lesovik, J. Math. Phys. **37**, 4845 (1996).
[14] G. B. Lesovik, F. Hassler, and G. Blatter, Phys. Rev. Lett. **96**, 106801 (2006).
[15] A. V. Lebedev, G. B. Lesovik, and G. Blatter, Phys. Rev. B **93**, 115140 (2016).
[16] G. B. Lesovik, M. V. Suslov, and G. Blatter, Phys. Rev. A **82**, 012316 (2010).
[17] M. V. Suslov, G. B. Lesovik, and G. Blatter, Phys. Rev. A **83**, 052317 (2011).
[18] J. Q. You and F. Nori, Nature **474**, 589 (2011).
[19] J. E. Mooij, T. P. Orlando, L. Levitov, L. Tian, C. H. van der Wal, and S. Lloyd, Science **285**, 1036 (1999).
[20] M. Bal, C. Deng, J.-L. Orgiazzi, F. R. Ong, and A. Lupascu, Nat. Commun. **3**, 1324 (2012).
[21] F. Yoshihara, K. Harrabi, A. O. Niskanen, Y. Nakamura, and J. S. Tsai, Phys. Rev. Lett. **97**, 167001 (2006).
[22] S. Danilin, A. V. Lebedev, A. Vepsäläinen, G. B. Lesovik, G. Blatter, and G. S. Paraoanu, arXiv:1801.02230.
[23] A. A. Abdumalikov, Jr., J. M. Fink, K. Juliusson, M. Pechal, S. Berger, A. Wallraff, and S. Filipp, Nature **496**, 482 (2013).
[24] K. S. Kumar, A. Vepsäläinen, S. Danilin, and G. S. Paraoanu, Nat. Commun. **7**, 10628 (2016).
[25] V. Giovannetti, S. Lloyd, and L. Maccone, Science **306**, 1330 (2004).
[26] P. Sekatski, M. Skotiniotis, J. Kolodynski, and W. Dür, Quantum **1**, 27 (2017).